$\zeta = z/\bar{\delta}$

τ = dimensionless time

LITERATURE CITED

1. Ludviksson, V., and E. N. Lightfoot, *AIChE J.*, *14*, 620 (1968).
2. Zuiderweg, F. J., and A. Harmens, *Chem. Eng. Sci.*, **9**, 89 (1958).
3. Francis, R. C., and J. C. Berg, *ibid.*, **22**, 685 (1967).
4. Brian, P. L. T., J. E. Vivian, and D. C. Matiatos, *AIChE J.*, **13**, 28 (1967).
5. Banerjee, S., E. Rhodes, and D. S. Scott, *Chem. Eng. Sci.*, **22**, 43 (1967).
6. Emmert, R. E., and R. L. Pigford, *ibid.*, **2**, 87 (1954).
7. Molstad, M. C., and L. F. Parsley, *ibid.*, **46**, 20 (1950).
8. Norman, W. S., and B. K. Soloman, *Trans. Inst. Chem. Eng.*, 37, 237 (1959).
9. Bond, J., and M. B. Donald, *Chem. Eng. Sci.*, **6**, 237 (1967).
10. King, P. J., and P. N. Walmsley, *J. Appl. Chem.*, **15**, 98 (1965).
11. Sternling, C. V., and L. E. Scriven, *AIChE J.*, **6**, 514 (1959).
12. Chu, J. C., S. L. Wang, S. L. Levy, and R. Paul, "Vapor-Liquid Equilibrium Data," J. W. Edwards, Ann Arbor, Mich. (1956).
13. Chu, J. C., R. J. Getty, L. F. Brennecke, and R. Paul, "Distillation Equilibrium Data," Rheinhold, New York (1950).

Manuscript received September 10, 1968; revision received March 25, 1971; paper accepted April 5, 1971.

An Experiment on Turbulent Diffusion in Additive Solutions

JIN WU

Hydronautics, Inc., Laurel, Maryland

Turbulent diffusion in high molecular weight additive solutions was measured and compared on a laboratory scale by observing the axisymmetric spreading of a cylindrical turbulent cloud in these solutions of various concentrations. Significant suppression of turbulence in additive solutions was observed. The trend of the results as a function of additive concentrations is similar to that of the additive reduction of turbulent frictional resistance.

The reduction of turbulent friction experienced by pumping additive solutions through pipes (*6*) seems to indicate the suppression of turbulence. However, it is held (*3, 10*) that these additive effects occur only in the region very close to the wall where the shear strain is high and the turbulence scale is small. These effects lead to a thickening of the viscous sublayer and consequently result in drag reduction. This argument, additive effects occurring only in the wall region, might discourage studies on free turbulent flow of additive solutions. However, the greatly suppressed advance of a turbulent front in additive solutions (*4, 11*) seems to evidence additive effects on turbulent diffusion. The present article includes the previously unpublished study (*11*) on the generation and the spreading of an axisymmetric, turbulent region in additive solutions. This result is important for estimating the diffusion of additive solutions ejected into a turbulent pure-water boundary layer.

EQUIPMENT AND EXPERIMENTAL TECHNIQUES

The turbulent cloud was generated by a spiral paddle in a transparent tank, 3 m. deep, 3 m. long, and 23 cm. wide. The paddle, shown in Figure 1*a*, was made by soldering screen sections to a rigid spiral frame, 5 cm. in diameter. Supported by a 0.9-cm. diam. perforated tube shaft, the paddle was connected to and controlled by a pendulum arrangement behind the tank. The paddle rotated about its axis as the pendulum swung outside the tank. Immediately prior to the test, a dye rod was inserted into a perforated tube. In several minutes the dye started to dissolve, and by then the turbulence created by the insertion of the dye rod was damped. The turbulent cloud was generated then by the spiral paddle with the pendulum swinging for a complete cycle, through a repeatable arc of 240 deg. The pendulum was released from the same position for all the tests and was caught on its back swing. The period of the generation is about 2 sec. With the help of dye being dissolved continuously into the cloud during the spreading process, the cloud boundary, although irregular, was distinctly visible, and was photographed by a movie camera. The cross section of the cylindrical cloud, during this photographing period (about 30 sec.), was radially symmetric generally; see Figure 1*b*. The radially symmetric shape indicates that an axisymmetrical flow is generated. The dark column shown in Figure 1*b* below the cloud was not generated by the paddle but was left there by dye dissolved from the dye rod.

In the present experiment, aqueous solution of polyox (polyethylene oxide, WSR-301) was selected as the testing medium. The concentrations for this additive were varied between 0 and 1,250 p.p.m.w.

This experimental technique was designed for studying, on a comparative basis, the turbulence-diffusion characteristics of additive solutions by observing the generation of a cylindrical turbulent cloud and its spreading in these solutions. During the generating process, large-scale eddies, having sizes comparable to the diameter of the paddle, were created by the frame of the paddle, while smaller ones, having sizes comparable to the void of the screen, were also excited. The total circulation introduced by the forward and backward swing of the paddle was virtually nil.

RESULTS

The process of diffusion of a cylindrical turbulent cloud in an undisturbed fluid consists of two different effects:

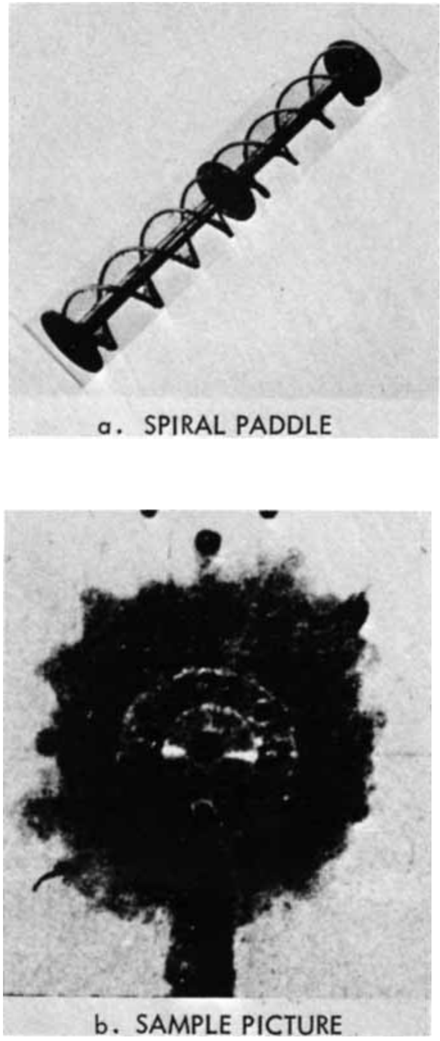

Fig. 1. Spiral paddle and sample picture of turbulent cloud.

molecular diffusion and eddy diffusion. The rate of molecular diffusion in polymeric solutions with low concentrations was found by Clough et al. (*1*) to be comparable with that of their solvents and, in the present experiment, is thus negligible compared to that of eddy diffusion.

As discussed previously, the generated cloud can be considered as a volume of fluid which consists of small eddies superimposed on large ones. However, once the turbulence, large- or small-scale, is excited by the paddle, nonlinear inertial effects in the fluid start to spread the energy over a wider range of the spectrum and particularly to transfer the energy to large wave numbers. Therefore the large eddies are continuously weakened at the expense of the small ones. The smallest eddies in the fluid are the principal agents of energy dissipation.

According to Townsend (*9*), there exists an irregular turbulent front which separates a fully turbulent region from the surrounding nonturbulent fluid. Along the front, the large eddies convect the fully turbulent fluid outward and simultaneously bring nonturbulent fluid inward; these eddies thus control the spreading rate of the turbulent region. The entrained fluid is immediately brought to a turbulent state due to the action of the small-scale turbulence at the expense of a continuous reduction of the turbulence level inside the cloud. In other words, this turbulent cloud can be considered as a field of turbulence with nearly uniform intensity except in the very narrow region close to the front.

The narrow region separating the turbulent and nonturbulent fluid, called the viscous superlayer by Corrsin and Kistler (*2*), consists of a thin layer in which the entrained, irrotational, nonturbulent fluid is transferred to a rotational, turbulent state by means of viscous shear. In addition, this layer advances with the front and remains thin, compared to the size of the cloud. Furthermore the turbulent velocities of the fluid particles in the front are proportional to those inside the cloud.

Based on all these arguments, the flow condition during spreading can be considered to be geometrically similar and the rate of advance of the turbulent front follows the expression

$$\frac{1}{u_0}\frac{dl_0}{dt} = \text{constant} \qquad (1)$$

where u_0 and l_0 are suitable velocity and length scales, which are functions of time only. For the present cylindrical cloud, l_0 and u_0 can best be represented by $\sqrt{\overline{r^2}}$ and $\sqrt{\overline{u'^2}}$, the root mean square radius of the cloud and the radial turbulent intensity, respectively. It follows from Equation (1)

$$\frac{1}{\sqrt{\overline{u'^2}}}\frac{d\sqrt{\overline{r^2}}}{dt} = \text{constant} \qquad (2)$$

wherein the constant, for a fully turbulent state, should be a universal one, independent of the flow medium.

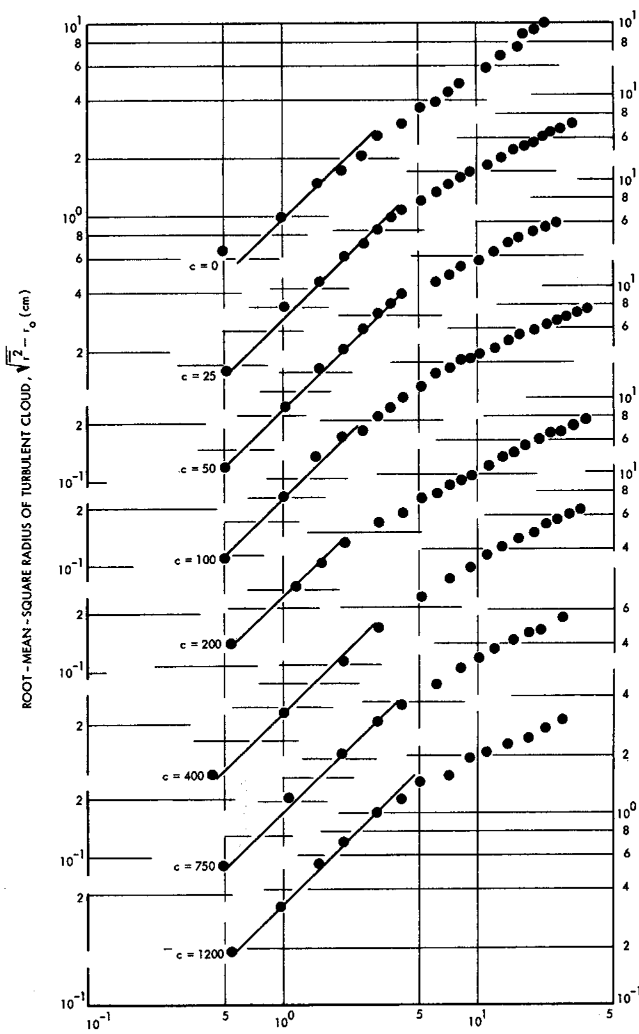

Fig. 2. Initial spreading of a turbulent cloud in polyox-additive solutions of various concentrations.

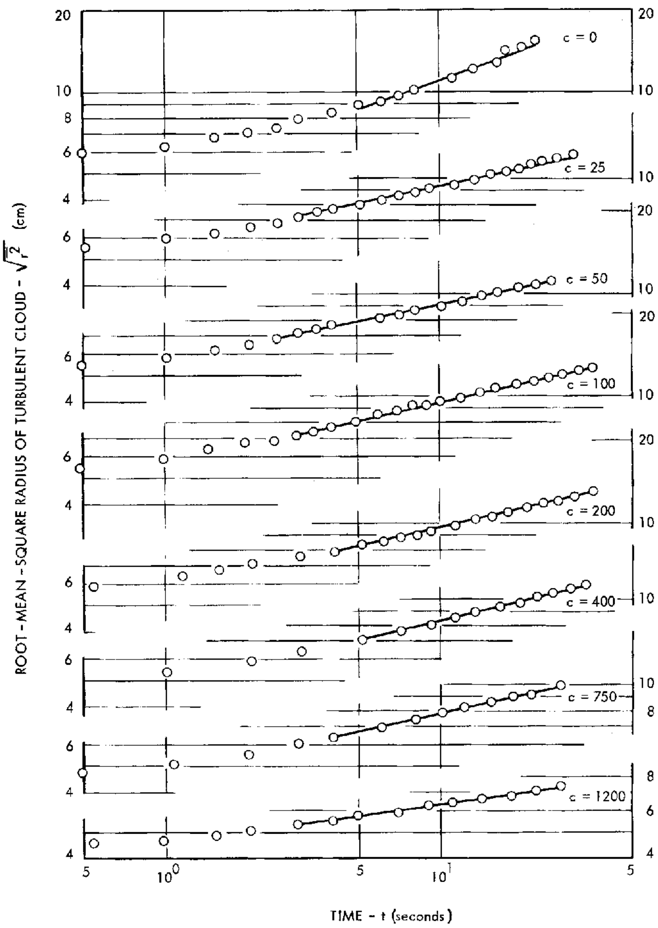

Fig. 3. Final spreading of a turbulent cloud in polyox-additive solutions of various concentrations.

The root mean square cloud radius can be calculated from the cloud area A, since

$$A = \sum_{i=1}^{N} \frac{r_i^2 \, \Delta\theta}{2} = \frac{\pi}{N} \sum_{i=1}^{N} r_i^2 \tag{3}$$

$$\sqrt{\sum_{i=1}^{N} r_i^2/N} = \sqrt{\overline{r^2}} = \sqrt{A/\pi} \tag{4}$$

The areas of the cloud were obtained by integrating the cloud profiles, traced from the film, with a planimeter. The distance between the movie camera and the tank is about 20 times the final size of the cloud. Consequently, optical distortion of the cloud profile is negligible.

These radii, $\sqrt{\overline{r^2}}$, obtained from tests in polyox solutions with various additive concentrations, are plotted separately in Figures 2 and 3. In the former figure the results were plotted differently adopting $\sqrt{\overline{r^2}} - r_0$ instead of $\sqrt{\overline{r^2}}$ to emphasize the initial spreading. In both figures r_0 is the initial root mean square radius of the turbulent cloud and c is the additive concentration.

DISCUSSION

Spreading of Turbulent Clouds

Periods of Diffusion. From the results shown in Figure 2, a straight line can fit the initial portion of data for each test. Viewing the data presented in Figure 3, one may draw a straight line through the last portion of the data. There is a time interval between these two fitted regions, corresponding to the period immediately following paddle-mixing and that of large t, respectively. The region shown in Figure 2 represents the initial period of diffusion, or period of turbulence generation, during which the turbulence is not decaying and the turbulent front advances at a nearly constant rate; the straight lines have unit slopes. The region shown in Figure 3 corresponds to the final period of diffusion, or period of turbulence decay, during which the turbulence is fully developed and the rate of advance of the turbulent front obeys a power law. Between these two periods of diffusion there appears a transition period.

Accepting these considerations, one may now compare the generation and decay of turbulence during the initial and final periods of spreading in various media.

Generation of Turbulence. For the initial period of spreading, a straight line of unit slope

$$\sqrt{\overline{r^2}} = at \tag{5}$$

was fitted, according to the least square principle, through the data. The intensity of the turbulence generated by the paddle mixing can be found from Equations (2) and (5).

$$\sqrt{\overline{u'^2}} = \text{constant} \cdot a \tag{6}$$

The values of a, obtained from tests with the same paddle mixing in additive solution of various concentrations, are shown in Table 1 and Figure 4*a*.

At the beginning of spreading, it may be assumed that the turbulent front consisted of the same fluid particles for a very short period and thus the initial spreading should obey the process of turbulent diffusion by continuous movement introduced by Taylor (*8*). For a homogeneous field with no mean motion, as in the present case, the diffusion law can be expressed as

$$\frac{d\overline{\eta^2}}{dt} = 2\,\overline{u'^2} \int_0^t R_L(\xi)\,d\xi \tag{7}$$

This standard deviation of the distance η traveled should be proportional to the root mean square cloud radius determined in the present experiment. When t is small so that the Langrangian correlation coefficient R_L will not differ appreciably from unity, one can obtain from Equation (7)

$$\eta = \sqrt{\overline{u'^2}}\,t \tag{8}$$

Based on the assumption of nondecaying turbulence for the initial period, Equation (8) is in agreement with the observed, temporally linear spreading of the turbulent cloud during the initial period.

Decay of Turbulence. As discussed previously, a power law can be found to represent the last portions of data, shown in Figure 3, or

$$\sqrt{\overline{r^2}} \sim t^n \tag{9}$$

where n is a numerical exponent which is the slope of

TABLE 1. EXPERIMENTAL RESULTS

Additive concentration, p.p.m.w.	Generation of turbulence a, cm./sec.	Decay of turbulence n	$1\text{-}n$
0	0.904	0.336	0.664
25	0.813	0.236	0.764
50	0.722	0.224	0.776
100	0.848	0.228	0.772
200	0.868	0.237	0.763
400	0.751	0.240	0.760
750	0.604	0.216	0.784
1,250	0.366	0.147	0.853

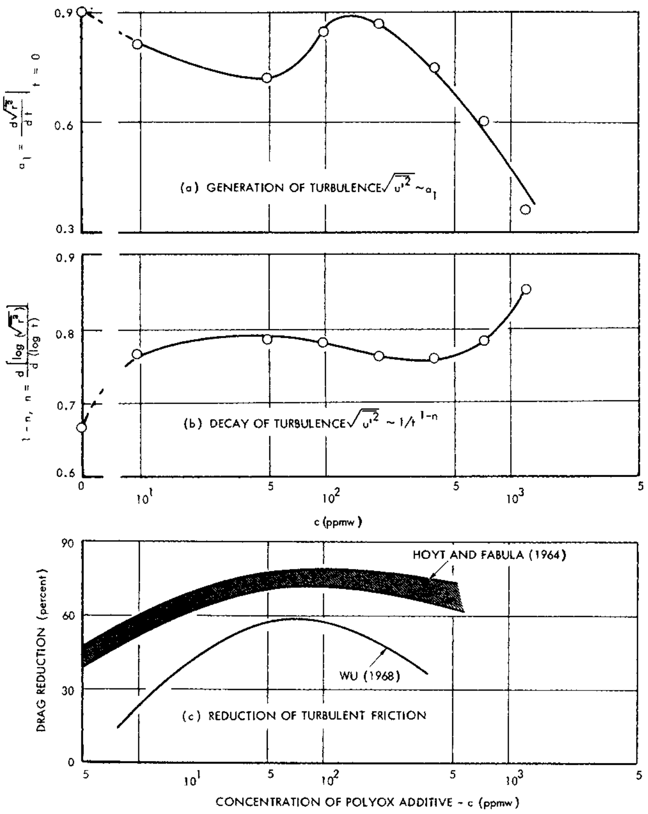

Fig. 4. Effects of polymer additive on suppression of turbulent diffusion and on reduction of turbulent friction.

straight-line segments shown in the same figure; see also Table 1.

From Equations (2) and (9), the rate of turbulence decay can be expressed as

$$\sqrt{u'^2} \sim \frac{1}{t^{1-n}} \tag{10}$$

Additive Effects on Suppressing Turbulent Generation and Entrainment

The effects of polyox additive on the generation of turbulence and on the suppression of turbulent entrainment (diffusion) are shown clearly in Figures 4*a* and 4*b*. The trends of these curves show that the minimum generation of turbulence and the maximum suppression of entrainment occur at an additive concentration near 50 p.p.m.w. The lower generation and stronger suppression of entrainment at higher additive concentrations, reversing the previous trend, are probably due to the rapidly increased fluid viscosity with additive concentrations. For a dilute polyox-additive solution, its viscosity increases almost linearly with the additive concentration and doubles its value at 900 p.p.m.w. (*7*).

The reduction of turbulent friction in pipe flows of polyox-additive solutions was reported by Hoyt and Fabula (*5*). The reduction of turbulent drag on a flat plat with the same kind solutions was studied by Wu (*12*). Their results, reproduced in Figure 4*c*, show a common maximum drag reduction at an additive concentration near 50 p.p.m.w. Since drag reduction depends on the Reynolds number, results different quantitatively from those presented in Figure 4*c* may be obtained. However, these data possess a common feature of having maximum drag reduction at a concentration in the neighborhood of 50 p.p.m.w. In other words, a close correlation of additive effects on drag reduction and on suppression of turbulence generation and of turbulent entrainment is exhibited.

CONCLUSIONS

The generation and decay of free turbulence in various testing media have been measured experimentally through analysis of the generation and of the spreading of a cylindrical cloud. The axisymmetric spreading of this cloud can be divided into two periods: The initial period, during which the turbulence is not decaying very much and the spreading obeys a simple linear law (cloud spreading linearly with time); and the final period, during which the turbulence has been fully developed and is decaying and the spreading obeys a simple power law.

Pure water and aqueous solutions of polyox additives of various concentrations were used as the test media. Significant changes in the generation and decay characteristics of free turbulence in the additive solutions with low concentrations were found. It is deduced that the polyox additive causes less generation and more decay of free turbulence than pure water. The effects of additives on the suppression of free turbulence seem to follow the same pattern of turbulent drag reduction.

ACKNOWLEDGMENT

I am indebted to M. P. Tulin for his suggestion of this study and supervision of the work. I am also grateful to J. Birkhead for his help in carrying out the experiment. This work was supported by the Office of Naval Research (Contract No. Nonr 4181 (00), NR 062-325).

NOTATION

a = turbulence intensity
A = area of spreading cloud
c = concentration (by weight) of additive in water
n = numerical exponent
l_0 = characteristic length scale
r = radius of spreading cloud
R_L = coefficient of Lagrangian correlation
t = time
$\sqrt{u'^2}$ = turbulence intensity
u_0 = characteristic velocity scale

Greek Letters

η = distance
ξ = time increment
$\Delta\theta$ = angular increment

LITERATURE CITED

1. Clough, S. B., H. E. Read, and A. B. Metzner, *AIChE J.*, 8, (3) (1962).
2. Corrsin, S., and A. L. Kistler, *NACA TN No. 3133* (1954).
3. Elata, C., J. Lehrer, and A. Kahanovitz, *Israel J. Technol.*, 3 (1) (1965).
4. Gadd, G. E., *Nature*, **212** (1966).
5. Hoyt, J. W., and A. G. Fabula, *Proc. 5th Symp. Naval Hydrodynamics* (1964).
6. Metzner, A. B., "Handbook of Fluid Dynamics," V. L. Streeter, Ed., Sec. 7, McGraw-Hill, New York (1961).
7. Rubin, H., and C. Elata, *Phys. Fluids*, 9 (10) (1966).
8. Taylor, G. I., *Proc. Roy. Soc. London*, **A15** (1933).
9. Townsend, A. A., "The Structure of Turbulent Shear Flow," Cambridge Univ. Press, London (1956).
10. Tulin, M. P., *Proc. 6th Symp. Naval Hydrodynamics* (1966).
11. Wu, Jin, *Hydronautics, Inc. Tech. Rept. 353-1* (1965).
12. ———, *Proc. Symp. Viscous Drag Reduction*, Dallas (1968).

Manuscript received January 4, 1971; revision received February 1, 1971; paper accepted February 3, 1971.